Growth-front roughening in amorphous silicon films by sputtering

T. Karabacak,* Y.-P. Zhao, G.-C. Wang, and T.-M. Lu
Department of Physics, Applied Physics and Astronomy, Rensselaer Polytechnic Institute, Troy, New York 12180-3590
(Received 14 February 2001; published 8 August 2001)

The growth-front roughness of amorphous silicon films grown by dc magnetron sputtering at low pressure has been investigated using atomic force microscopy. The interface width w increases as a power law of deposition time t, $w \sim t^{\beta}$, with $\beta = 0.41 \pm 0.01$, and the lateral correlation length ξ grows as $\xi \sim t^{1/z}$, with $1/z = 0.42 \pm 0.02$. The roughness exponent extracted from height-height correlation analysis is $\alpha = 0.83 \pm 0.03$. None of the known growth models can be used to explain the scaling exponents we obtained. Monte Carlo simulations were carried out based on a re-emission model where incident flux distribution, sticking coefficient, and surface diffusion were accounted for in the growth process. The morphology and the scaling exponents obtained from simulations are consistent with the experimental results. When the surface diffusion is switched off in the simulation, columnar structures begin to appear and this is also consistent with the experimental observations of other authors

DOI: 10.1103/PhysRevB.64.085323 PACS number(s): 68.55.−a, 68.47.−b, 81.15.−z

I. INTRODUCTION

Thin-film growth is a very complicated stochastic process. Thin-film growth fronts under nonequilibrium conditions often show scaling behaviors, and have attracted considerable interest.[1–3] Dynamic scaling exponents are used to characterize the morphology change of the growing film. Theoretical studies show that depending on the growth mechanism a number of distinct universality classes can be defined, each having a different set of scaling exponents. Therefore from the scaling exponents one may learn what type of processes are involved during the growth. However, experimental conditions are often more complicated and the scaling exponents obtained are often different from those predicted theoretically.[2] This has stimulated researchers to find new models that are more realistic and closer to the actual experimental conditions.[4,5]

Silicon has been a widely used material in the semiconductor industry and is a material of special interest. The dynamic roughening of silicon thin films grown by thermal evaporation,[6,7] chemical vapor deposition,[8] and molecular-beam epitaxy[9–12] were studied in the past. The reported scaling exponents basically depend on the deposition technique used. Although some morphological properties of sputter deposited Si films were reported,[13,14] a detailed dynamic growth study for silicon films grown by sputtering has not been carried out. In this paper, we present measurements of the growth-front roughness of amorphous silicon films grown by a dc magnetron sputtering system. Amorphous films simplify the growth process, because the Schwoebel barrier effect is not believed to play an important role.[6,7] We extract the scaling exponents and suggest a re-emission model to describe the possible surface growth mechanisms during sputter deposition. Different than the re-emission model proposed by Jason *et al.*,[4,5] the model we used takes into account surface diffusion and has a more directional incident flux of particles compared to the one used in their work.

II. EXPERIMENT AND RESULTS

Amorphous silicon (a-Si) films were deposited on Si(100) substrates in a CVC© magnetron sputter deposition system. Sputtering was performed with a high-purity Si target in an Ar working gas. A background pressure of 3.0×10^{-6} Torr was generated in the sputtering chamber prior to the Si deposition. The target was water cooled and the substrate holder was neither cooled nor initially heated. Substrate temperature during the depositions was approximately 70–80 °C. Amorphous Si films were deposited in a 5-mTorr argon pressure and the dc discharge power was 900 W (2.81 W/cm^2 for our geometry). Presputtering was performed for cleaning the Si target surface before the sputtering of silicon. Films were grown at deposition times varying from 5 min up to 10 h. The growth rate was measured to be $R \simeq 10.7 \pm 0.5$ nm/min. *Ex situ* x-ray-diffraction (XRD) measurements revealed the amorphous structure of the films. Cross-sectional scanning electron microscopy (SEM) measurements showed no columnar structure unlike that observed by Unagami *et al.* in their sputter deposited a-Si films at higher Ar pressure (~30 mTorr).[13]

The quantitative information of the surface morphology can be extracted from the equal-time height-height correlation function $H(\mathbf{r},t)$, defined as $H(\mathbf{r}) = \langle [h(\mathbf{r}) - h(\mathbf{0})]^2 \rangle$. Here $h(\mathbf{r})$ is the surface height at position $\mathbf{r}[=(x,y)]$ on the surface relative to the mean surface height. The notation $\langle \cdots \rangle$ means a statistical average. The scaling hypothesis requires that $H(r) \sim r^{2\alpha}$ for $r \ll \xi$, and $H(r) = 2w^2$ for $r \gg \xi$.[1–3] Here ξ is the lateral correlation length, w is the interface width or rms roughness, and α is the roughness exponent, which describes the surface fractality. The interface width w increases as a power law of growth time t, $w \sim t^{\beta}$, where β is the growth exponent, and the lateral correlation length ξ grows as $\xi \sim t^{1/z}$, where $1/z$ is the dynamic exponent. Dynamic scaling also requires that $z = \alpha/\beta$. Therefore, from the slopes of linear fits to the log-log plots of $H(r)$ versus r (for $r \ll \xi$), w versus t, and ξ versus t, we can extract the roughness exponents α, β, and $1/z$, respectively.

 ©2001 The American Physical Society

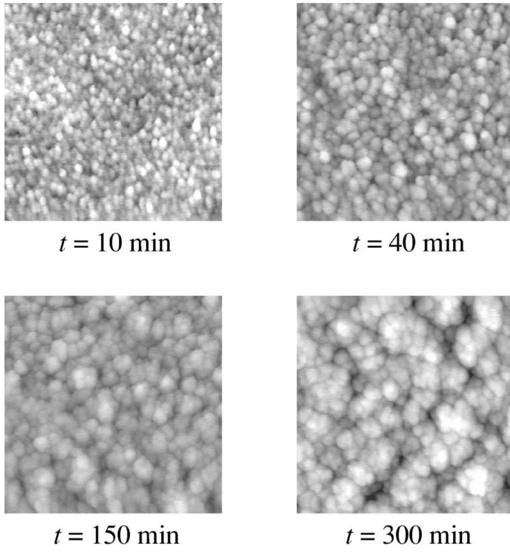

FIG. 1. Some representative surface images ($1\times1\ \mu m^2$) of amorphous Si films measured by AFM for growth times of $t=10$, 40, 150, and 300 min.

The surface morphology was measured using contact-mode AFM (atomic force microscopy) (Park Scientific Auto CP). The radius of the Si_3N_4 tip is about 10 nm, and the side angle is about 10°. Each AFM image included 256×256 pixels. Representative surface morphologies are shown in Fig. 1 for the growth times of $t=10$, 40, 150, and 300 min. As one can see from Fig. 1, the surface features grow with time.

In Fig. 2 we plot the height-height correlation function $H(r,t)$ curves in log-log scale for different deposition times. These curves were obtained by using a line-by-line averaging process. The line-by-line and circular averaging methods give the same result due to the isotropic nature of the films. All the $H(r,t)$ do not overlap each other until the deposition times reach around 20 min. Up to 20 min the growth is nonstationary. In other words, the local surface slope is a function of growth time.[15] In a nonstationary growth the scaling relation $z=\alpha/\beta$ may break down.[16] After 20 min, the height-height correlation curves begin to overlap, which suggests that the growth, after 20 min, gradually becomes stationary. The roughness exponent value of each $H(r,t)$ curve is the same within the experimental errors: $\alpha=0.83\pm0.03$. But measured α values can be higher than the true values because of the tip effect.[17] Aue *et al.* showed that the surface fractal dimension determined with a scanning probe technique will always lead to an underestimate of the actual scaling dimension, due to the convolution of tip and surface [fractal dimension d_f for a $1+1$ interface is related to α by $d_f=2-\alpha$ (Ref. 2)]. Aue *et al.* analysis included tips with different shapes and aspect ratios. Their analysis for a tip similar to what we used suggests that our true α should be around 0.6–0.7.

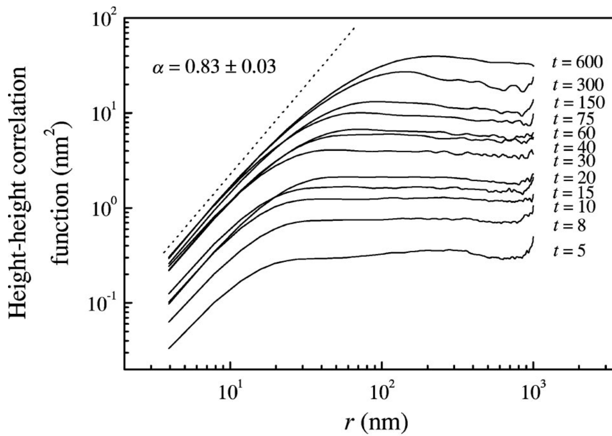

FIG. 2. The equal-time height-height correlation function $H(r,t)$ as a function of the distance r is plotted in log-log scale. The unit of growth time t labeled near each $H(r,t)$ curve is minutes. Each $H(r,t)$ within the short-range spatial scaling regime gives the same α value indicated as the dashed line.

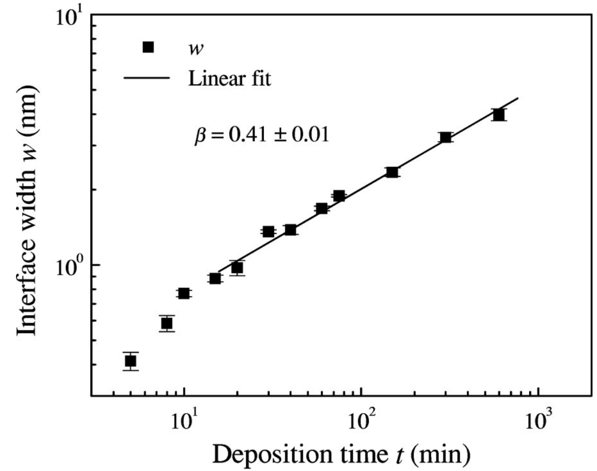

FIG. 3. The interface width w versus growth time t is plotted in log-log scale. The best linear fit gives the growth exponent β.

The interface width w as a function of deposition time t is plotted in Fig. 3. The linear fit to Fig. 3 gives the growth exponent $\beta=0.41\pm0.01$. In this fit we did not include data points up to $t=20$ min, because the slope in this regime is pretty high ($\beta\simeq0.71$) suggesting that growth is random here. In order to determine ξ accurately, we calculated the two-dimensional autocorrelation $C(\mathbf{r})=\langle h(\mathbf{r})h(\mathbf{0})\rangle$ function from each AFM image, and use the quadrant circularly averaged autocorrelation function $C_c(\mathbf{r})$ to determine ξ by the relation $C_c(\xi)=C_c(0)/e$. The log-log plot of ξ versus t is shown in Fig. 4. As can be seen from Fig. 4, ξ does not change too much up to the deposition times $t=20$ min, after which a stationary growth begins to develop. On the other hand, after 20 min the lateral correlation increases linearly in the log-log plot, and the best fit to this regime gives $1/z=0.42\pm0.02$ ($z=2.38\pm0.11$). From the measured α and β, the scaling relation $z=\alpha/\beta$ predicts $1/z\simeq0.49$ ($z\simeq2.02$), which is close to the measured $1/z$.

III. DISCUSSION

A. Growth model

Our experimental results show that the roughness exponents obtained for our sputter deposited silicon films fit none

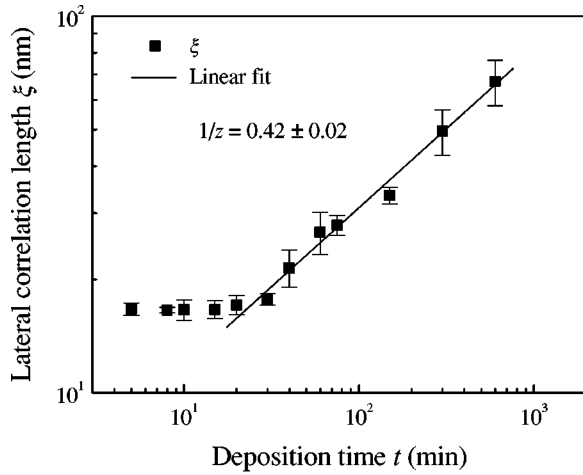

FIG. 4. The lateral correlation length ξ versus growth time t is plotted in log-log scale. The best linear fit gives the dynamic exponent $1/z$.

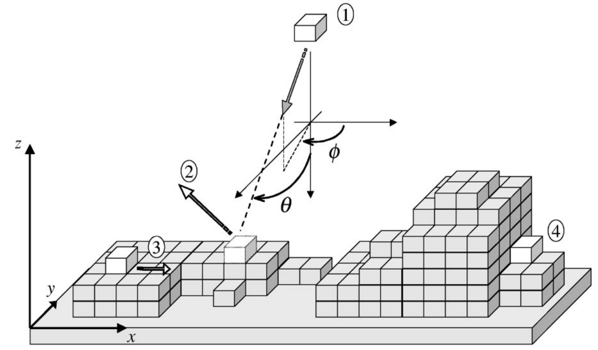

FIG. 5. Some basic processes in the Monte Carlo simulation: (1) A particle is sent towards surface with angles θ and ϕ. This particle sticks to the surface with probability s_0. (2) If the particle does not stick, then it is re-emitted. If it finds another surface feature on its way it may stick there with probability s_1. The re-emission process goes on like this for higher-order particles, too. (3) An adatom can diffuse on the surface. (4) Some surface points are shadowed from the incident and re-emission fluxes of particles due to the nearby higher surface features.

of the presently known universality classes.[1–3] Local models typically give $\beta \leqslant 0.25$ except the random deposition model where $\beta = 0.50$. In a local growth model, each surface point is related only to a limited number of neighboring points. In reality, the morphology of the neighboring points can result in a shadowing effect where the valleys of the surface receive less incident flux due to the hills around them. A pure shadowing effect would give $\beta = 1$.[5,18,19] Furthermore, an incident atom can bounce off of the surface depending on its sticking coefficient (s_c). The average probability of sticking is a result of the complicated interactions between the incident atom and the surface. These re-emitted particles can fill the valleys faster and increase the conformality. Another smoothening effect comes from adatom diffusion on the surface towards regions with lower surface potential energy (e.g., valleys), which is a local effect.

We suggest that the recently developed re-emission model by Drotar *et al.*[4,5] can bring out a good degree of explanation of the surface dynamics of our sputter growth results. The model assumes a two-dimensional surface described by a height function $h(\mathbf{r},t)$. Overhangs are not allowed. The ratio of the mean free path of the incoming particles to the characteristic length of the surface features is assumed to be large (Knudsen number $\gg 1$) which is the case in our experiment. Hence collisions between particles within the surface features are neglected. It is also assumed that the surface evolves slowly compared to the redistribution of flux due to the surface features (e.g., within the time it typically takes for a re-emitted particle to go from one point on the surface to another, the surface does not change much). The probability of an incoming particle sticking to the surface is s_0 ($0 \leqslant s_0 \leqslant 1$), where s_0 is called the zeroth-order sticking coefficient. Incoming particles are called zeroth-order particles, while an nth-order particle that has been re-emitted is called an $(n+1)$th-order particle. The probability of an nth-order particle sticking is s_n ($0 \leqslant s_n \leqslant 1$), and if the particle does not stick (this has a probability $1-s_n$), then it will be re-emitted (in other words, the flux is redistributed). The overall flux of nth-order particles at the in-plane position $\mathbf{r}$ at time t is denoted by $F_n(\mathbf{r},t)$. A detailed description of the characteristics of F_n and the concept of the re-emission mode is given in Ref. 4. The proposed growth model has the form

$$\frac{\partial h}{\partial t} = \nu \nabla^2 h - \kappa \nabla^4 h + \sqrt{1+(\nabla h)^2}[s_0 F_0(\mathbf{r},t) + s_1 F_1(\mathbf{r},t) + \cdots] + \eta, \tag{1}$$

where the first, second, and last terms are the condensation/evaporation, surface diffusion, and noise terms, respectively. The inherent noise in the growth process satisfies

$$\langle \eta(\mathbf{r},t) \rangle = 0, \text{ and} \tag{2}$$

$$\langle \eta(\mathbf{r},t)\, \eta(\mathbf{r}',t') \rangle = 2A\, \delta(\mathbf{r}-\mathbf{r}')\, \delta(t-t'), \tag{3}$$

where A is proportional to the root-mean-square value of the noise term. The factor $\sqrt{1+(\nabla h)^2}$ in Eq. (1) implies that the growth takes place normal to the surface. The main difficulty lies in finding each F_n. An analytical form of F_n has been proposed that takes into account re-emission modes and shadowing effects.[4,5]

B. Numerical calculations

Numerical computation times of Eq. (1) are quite long for a reasonable scaling regime. Instead, we used Monte Carlo code to simulate growth corresponding to that given by Eq. (1). The details of the basic processes used in the code are given in Refs. 4 and 5. We took into account surface diffusion in our simulations, which was not included in Refs. 4 and 5 before. A summary of basic growth processes is sketched in Fig. 5. Briefly, the simulation proceeds according to a simple set of rules. A single particle (with a position described by *x, y*, and *z*) is introduced with random (uniformly distributed) variables *x* and *y*, while *z* is set to the maximum height of the surface, plus 1. The direction of the particle follows the distribution $dP(\theta,\phi)/d\Omega$

$=(2\cos\theta)/(\pi\sin\theta)$, where ϕ is the angle of the projection of the particle's trajectory in the xy plane, θ is the angle between the particle's trajectory and the negative z axis, and $d\Omega$ is equal to $d(\cos\theta)d\phi$. We believe that this type of flux distribution can represent a typical flux of sputtered atoms.[20,21] We used a square lattice surface model which is much faster than off-lattice models and can equivalently simulate amorphous structures.[2,3] The particle moves in a straight line until it hits the surface and it is either deposited ($h \rightarrow h+1$) or is re-emitted according to the thermal re-emission mode. The particle then travels in a straight line until it hits the surface again or heads away from the surface (in other words, z equals the maximum of the surface plus 1). The particle is allowed to continue "bouncing" off the surface until it is deposited on the surface or heads away from the surface.

Once a particle is deposited, a prescribed number of atoms, being set to D/F, are randomly picked to become candidates for diffusion. Here, D denotes the number of surface atoms that are available to diffuse within the unit time interval, in which F atoms are deposited to the surface. Therefore, at a time step of a deposited single particle ($F=1$), the surface can, at most, have D/F diffusing atoms. In this way, the ratio of diffusion to deposition strength is adjusted (see the discussion given on p. 176 of Ref. 2). The diffusing surface atom can jump to a nearby site with a probability proportional to $\exp[-(E_0+nnE_N)/k_BT]$. Here E_0 is the activation energy for diffusion, E_N is the bonding energy with a nearest neighbor, and nn is the number of nearest neighbors. k_B and T are the Boltzmann constant and surface temperature, respectively. The particle goes on jumping until it finds an island of atoms, a kink site, a valley or any lattice point, where (E_0+nnE_N) becomes large and the diffusion probability becomes small. The diffusing particle is prohibited from making a single jump up to a site where the height change is more than one lattice atom. But it can diffuse all the way down to surface valleys at any time (i.e., $\Delta h \leqslant 1$). We set the evaporation/condensation terms to zero in our code, since we believe that these effects become negligible at low substrate temperatures (see Chaps. 13 and 14 of Ref. 2). Finally, after the diffusion step is done, another particle is allowed to fall on the surface and the whole process is repeated. We note that our incident flux distribution is different from the one used in Refs. 4 and 5. In addition, we include surface diffusion.

During the simulations, we used a 1024×1024 lattice size for the surface in the x and y plane. We first considered a pure shadowing case and set $s_0=1$.[5] Without the surface diffusion our simulations gave $\beta \simeq 1$ with a highly columnar surface morphology, which was not observed in our experiment. Then, the diffusion parameters were set to $E_0=0.1$ eV, $E_N=0.1$ eV, and $T=350$ K with D/F values varying from 10 to 60. We still got $\beta \simeq 1$ with a similar columnar morphology. More realistically, the value of s_0 should be less than 1. Assuming that the incident silicon atoms have energies in the range of 1–10 eV,[20,22] we estimated that s_0 is between 0.56 and 0.76 by simulations[23] and $s_{n>0} \simeq 1$. Simulations with $s_0=0.65$, $s_{n>0}=1$ and without surface diffusion gave $\beta=0.67\pm0.02$ and $\alpha=0.50\pm0.01$. We then activated

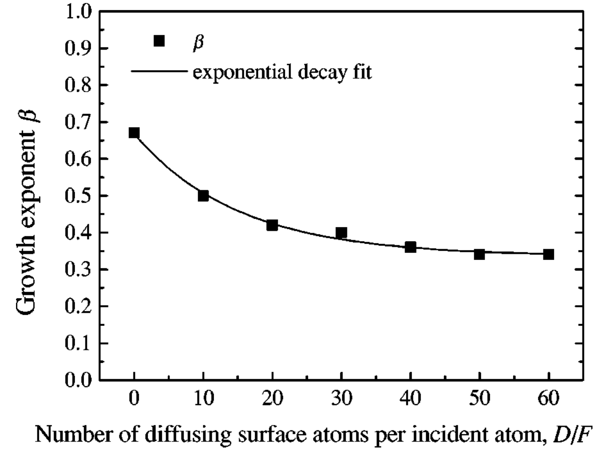

FIG. 6. The change of growth exponent β as the number of atoms to diffuse on the surface per incident atom (D/F) is increased. We set $s_0=0.65$ and $s_{n>0}=1$ during the simulations. The simulated data were also fit by an exponential decay curve. The fit gives $\beta \rightarrow 0.34$ as $D/F \gg 0$.

the surface diffusion and increased the D/F values up to 60. The adatom diffusion is believed to originate from the localized temperature spikes at the vapor-solid interface due to the argon ion bombardment.[13,24] This effect is enhanced as the working pressure of argon is decreased.[13]

The change of the growth exponent β with D/F is shown in Fig. 6. As can be seen from Fig. 6, as D/F gets higher, β converges to the value ~0.34. In this range of high D/F the roughness exponent approaches $\alpha \simeq 0.38$. (The scaling exponents are very sensitive to the value of s_n and partially to D/F. For some s_n values, the scaling exponents do not change significantly with the increase of D/F.[25]) At $D/F=20$ we obtain $\beta=0.42\pm0.02$, $\alpha=0.44\pm0.01$, and $1/z=0.67\pm0.04$ ($z=1.49\pm0.09$).

Figure 7 shows the surfaces obtained from the simulations with $s_0=0.65$, $s_{n>0}=1$, and $D/F=20$. These simulated morphologies are very similar to the AFM pictures shown in Fig. 1. Height-height correlation function evolution obtained from the morphologies at various deposition times are plotted in Fig. 8(a). The interface width after a long simulation was shown in Fig. 8(b). As can be seen from Fig. 8(b), the log-log plot of interface width has a linear part, from which we extract β at intermediate times denoted by arrows. Figure 8(b) also shows that at longer times the interface width reaches a saturation point after which it does not increase anymore. The growth exponent β obtained from simulations 0.42 ± 0.02 agrees well with experimental value 0.41 ± 0.01. The roughness exponent α from the experiments 0.83 ± 0.03 is higher than 0.44 ± 0.01 predicted above. However, the true α value after the corrections due to the finite tip effect is expected to be lower than the experimental α. Using the analysis by Aue *et al.* we estimated the true α to be around 0.6–0.7. The dynamic exponent $1/z$ from the experiments 0.42 ± 0.02 is lower than 0.67 ± 0.04 obtained from the simulations. Taking into account the tip effect, by using a corrected $\alpha\sim0.65$ we obtained the dynamic exponent from the scaling relation $z=\alpha/\beta$ to be $1/z \simeq 0.63$, which is close to the simulations.

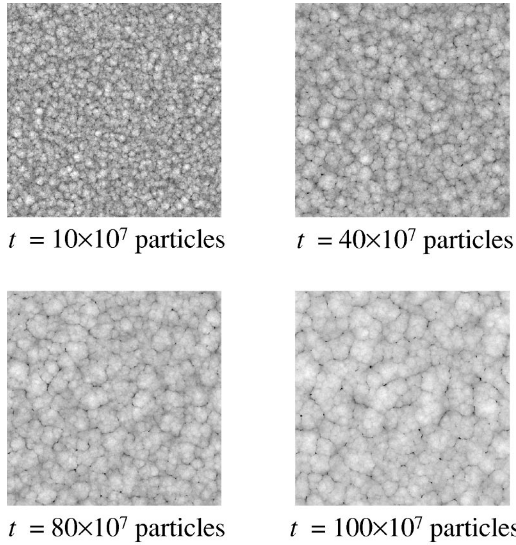

FIG. 7. Surface morphologies obtained by the re-emission model with $s_0=0.65$, $s_{n>0}=1$, and $D/F=20$ for growth times of $t=10$, 40, 80, and 100×10^7 particles. The pictures correspond to 512×512 subregions of the simulated surfaces.

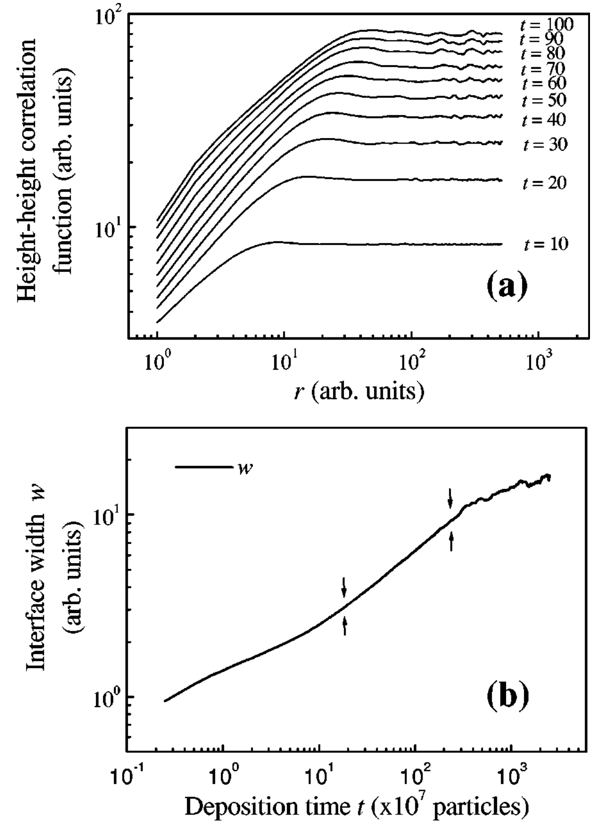

FIG. 8. (a) The equal-time height-height correlation function $H(r,t)$ curves obtained from the simulated surfaces with $s_0=0.65$, $s_{n>0}=1$, and $D/F=20$ as a function of the distance r are plotted in log-log scale. The unit of growth time t labeled near each $H(r,t)$ curve is ($\times10^7$ particles.). (b) The interface width w versus growth time t is plotted in log-log scale. β is extracted from the linear part of the plot indicated by arrows after which w reaches the saturation level.

Unagami *et al.* observed that as the argon gas pressure is increased, the self-bias potential on the substrate is reduced, and the average energy of the ion bombardment is reduced.[13] They observed that the overall effect of this increase of argon pressure was to enhance the columnar structure formation. They suggest that at higher argon pressures, the incident silicon atoms are scattered more efficiently, and the oblique component of the incident Si flux is more pronounced. This results in more shadowing effects and therefore more significant columnar structures. We believe that the model we presented above can also be used to describe the enhanced columnar structure formation. As mentioned above the decrease of self-biasing at higher Ar gas pressures would reduce the energy of ions bombarding the surface. Lower energy ions would reduce the effect of localized temperature spikes,[24] and therefore would reduce the diffusion of surface atoms. This corresponds to lower D/F values, and therefore higher β values and more pronounced columnar morphologies.

IV. CONCLUSIONS

In conclusion, the dynamic growth front roughening of a-Si films prepared by a low-pressure magnetron dc sputtering system was presented. SEM pictures showed no columnar structures. Morphology of the films at different deposition times was measured using AFM. A scaling hypothesis has been used to describe the measured exponents $\alpha=0.83\pm0.03$, $\beta=0.41\pm0.01$, and $1/z=0.42\pm0.02$. None of the well-known growth models describes the scaling exponents we obtained. We used a re-emission model having a nonlocal nature to describe our results. The model includes the re-emission of particles, surface diffusion, and uncorrelated noise effects. For faster computation times, we used Monte Carlo code to simulate the growth process. Simulations with a high directionality flux, a first-order re-emission process, and surface diffusion gave $\alpha=0.44\pm0.01$, $\beta=0.42\pm0.02$, and $1/z=0.67\pm0.04$. The growth exponent β agrees very well with the experimental result. The higher and the lower values of the experimentally obtained α and $1/z$, respectively, can be attributed to the AFM tip artifact. If the tip effect is considered, the α value is estimated to be ~0.65 and the $1/z$ value increases to ~0.63, close to the simulated 0.67 ± 0.04. As the surface diffusion is removed from the simulation, columnar structures begin to appear and this is also consistent with the experimental observations of others.

ACKNOWLEDGMENTS

We thank J. T. Drotar for helpful discussions. T. K. was supported by the Harry F. Meiners Program. This work is supported in part by NSF.

*Electronic address: karabt@rpi.edu

[1] F. Family and T. Vicsek, *Dynamics of Fractal Surfaces* (World Scientific, Singapore, 1991).
[2] A.-L. Barabási and H. E. Stanley, *Fractal Concepts in Surface Growth* (Cambridge University Press, Cambridge, England, 1995).
[3] P. Meakin, *Fractals, Scaling, and Growth Far from Equilibrium* (Cambridge University Press, Cambridge, England, 1998).
[4] J. T. Drotar, Y.-P. Zhao, T.-M. Lu, and G.-C. Wang, Phys. Rev. B **61**, 3012 (2000).
[5] J. T. Drotar, Y.-P. Zhao, T.-M. Lu, and G.-C. Wang, Phys. Rev. B **62**, 2118 (2000).
[6] H.-N. Yang, Y.-P. Zhao, G.-C. Wang, and T.-M. Lu, Phys. Rev. Lett. **76**, 3774 (1996).
[7] M. Lütt, J. P. Schlomka, M. Tolan, J. Stettner, O. H. Seeck, and W. Press, Phys. Rev. B **56**, 4085 (1996).
[8] T. Yoshinobu, A. Iwamoto, K. Sudoh, and H. Iwasaki, in *Fractal Aspects of Materials*, edited by F. Family, P. Meakin, B. Sapoval, and R. Wool, Mater. Res. Soc. Symp. Proc. **367** (Materials Research Society, Pittsburgh, 1995), p. 329.
[9] D. J. Eaglesham and G. H. Gilmer, in *Proceedings of the Workshop on Surface Disordering: Growth, Roughening, and Phase Transitions*, edited by R. Jullien, J. Kertesz, P. Meakin, and D. E. Wolf (Nova Science, New York, 1992), p. 69.
[10] H.-N. Yang, G.-C. Wang, and T.-M. Lu, Phys. Rev. Lett. **73**, 2348 (1994).
[11] P. H. Hegeman, H. J. W. Zandvliet, G. A. M. Kip, and A. van Silfhout, Surf. Sci. **311**, L655 (1994).
[12] O. P. Karpenko, S. M. Yalisove, and D. J. Eaglesham, J. Appl. Phys. **82**, 1157 (1997).
[13] T. Unagami, A. Lousa, and R. Messier, Jpn. J. Appl. Phys., Part 2 **36**, L737 (1997).
[14] G. F. Feng, M. Katiyar, Y. H. Yang, J. R. Abelson, and N. Maley, in *Microcrystalline Semiconductors: Materials Science & Devices*, edited by P. M. Fauchet, C. C. Tsai, L. T. Canham, I. Shimizu, and Y. Aoyagi, Mater. Res. Soc. Symp. Proc. **283** (Materials Research Society, Pittsburgh, 1993), p. 501.
[15] T.-M. Lu, H.-N. Yang, and G.-C. Wang, in *Fractal Aspects of Materials* (Ref. 8) p. 283.
[16] Y.-P. Zhao, G.-C. Wang, and T.-M. Lu, *Characterization of Amorphous and Crystalline Rough Surfaces: Principles and Applications* (Academic Press, San Diego, 2000).
[17] J. Aue and J. Th. M. De Hosson, Appl. Phys. Lett. **71**, 1347 (1997).
[18] R. P. U. Karunasiri, R. Bruinsma, and J. Rudnick, Phys. Rev. Lett. **62**, 788 (1989).
[19] J.-H. Yao and H. Guo, Phys. Rev. E **47**, 1007 (1993).
[20] K. Wasa and S. Hayakawa, *Handbook of Sputter Deposition Technology* (Noyes Publications, Park Ridge, NJ, 1992), Chap. 3.
[21] T. S. Cale and V. Mahadev, in *Modeling of Film Deposition for Microelectronic Applications*, Thin Films, Vol. 22, edited by S. Rossnagel and A. Ulman (Academic, San Diego, 1996), p. 175.
[22] Z. He, S. Inoue, G. Carter, H. Kheyrandish, and J. S. Colligon, Thin Solid Films **260**, 32 (1995).
[23] We used a molecular-dynamics code Simulation Kit Version 2.3 written by M. A. Karolewski at Nanyang Technological University, Singapore. Also, D. N. Ruzic from University of Illinois at Urbana-Champaign suggested similar sticking coefficients in our private communications.
[24] R. F. Bunshah and R. S. Juntz, J. Vac. Sci. Technol. **9**, 1404 (1972).
[25] T. Karabacak, Y.-P. Zhao, G.-C. Wang, and T.-M. Lu (unpublished).